Autonomous Navigation Using Bio-inspired Soft Tactile Sensors for Close-Proximity Perception

Emre Ozturk[1], Ismail Uyanik[1], and Solen Kumbay Yildiz[1]

***Abstract*— This paper presents a low-cost, bio-inspired soft robotic antenna designed for close-proximity depth sensing, modeled after the tactile functionality of insect antennae. Fabricated from a flexible silicone rubber substrate with embedded microchannels containing conductive carbon paste, the sensor utilizes resistance-based feedback to estimate distance. The sensor's performance is characterized through time-domain analysis and modeled using a fifth-order recursive least squares estimation (RLSE) algorithm. The effectiveness of the soft antenna is demonstrated through an autonomous wheeled robot executing Bug1, Bug2, and TangentBug algorithms for wall-following and obstacle avoidance. Results show that the soft antenna provides reliable distance sensing and accurate obstacle detection, offering a resilient and scalable solution for bio-inspired perception in autonomous systems.**

I. INTRODUCTION

Tactile sensing is fundamental to the navigation and movement capabilities of many animals, enabling them to interact with their surroundings through specialized sensory organs. In nature, animals rely on neuromasts, tactile hairs, and subcutaneous receptors to process environmental feedback via their central nervous systems [1]. Among these, the antennae of arthropods—including crustaceans and insects—serve as highly specialized tactile sensors, equipped with dense sensory hairs that facilitate crucial functions such as distance perception, route planning, leg coordination, and goal-directed motion [2]. These biological structures are not only active tools for exploration but also function as passive sensors, as seen in wall-following behavior, a critical survival mechanism for many species [3], [4]. Understanding these natural sensing mechanisms provides valuable insights for designing robotic systems that can operate efficiently in unstructured environments.

The study of biological sensory feedback has led to significant advancements in bio-inspired robotics, with researchers developing robotic systems that mimic the locomotion of various animals, including arthropods, fish, and reptiles [5]–[8]. In parallel, recent developments in soft robotics have introduced compliant structures that function as both actuators and sensors, offering increased adaptability and resilience in robotic designs [9]–[11]. Inspired by the wall-following behavior of the American cockroach (*Periplaneta americana*), this study proposes a low-cost soft robotic antenna for close-proximity sensing. Designed as a flexible and compliant alternative to conventional rigid sensors, the antenna detects resistance changes during bending, providing an effective and biologically inspired solution for tactile perception in robotics.

While previous research has explored passive antenna designs and robotic systems replicating cockroach wall-tracking behavior [12]–[14], these approaches have primarily relied on rigid components — passive mechanical deflection elements [12], potentiometers and capacitive contact sensors [13], [14] — with well-established physical models for distance measurement. Recent advances have demonstrated soft and flexible electronic antennas for tactile perception [15], [16] and contact-based tactile navigation using compliant structures [17]; however, these systems either stop short of full closed-loop reactive navigation or rely on supplementary sensing modalities for path planning. In contrast, soft sensors fabricated from stretchable elastomers offer greater flexibility and resilience but present significant challenges for closed-loop control. Prior work has addressed this through neural network-based approximated models [18] and reduced-order finite element model observers [19]; however, these approaches require either computationally expensive offline model construction or retraining under new conditions, limiting their deployment on resource-constrained mobile platforms. Furthermore, existing compliant antenna designs — such as [20] — embed rigid sensing elements (e.g., flex sensors) within a soft body structure, rather than using purely soft transduction material throughout. This distinction matters: a rigid sensing element imposes mechanical constraints on the antenna's bending profile, introduces discrete measurement artifacts, and ultimately limits the compliance that motivates soft sensor design in the first place. The sensor proposed in this work occupies a different point in the design space: a fully soft, microfluidic construction in which conductive carbon paste fills elastomeric microchannels, enabling continuous resistance-based distance estimation with no rigid sensing elements and no external actuation. This architecture eliminates the mechanical constraints of hybrid designs while remaining amenable to lightweight mathematical modeling via system identification, as demonstrated in the following sections.

This work builds upon prior sensor characterization [21] by refining its modeling through a recursive least squares estimation (RLSE) algorithm [22] and integrating it with Bug algorithms — reactive path-planning strategies for navigating unknown environments [23], [24]. Bug algorithms have been widely studied as a benchmark for evaluating reactive navigation strategies, with comparative analyses demonstrating that their performance is particularly sensitive to the quality

*This work was supported by the Scientific Research Projects Coordination Unit of Hacettepe University (Grant No. FHD-2022-19964)

[1]All authors are with the Department of Electrical and Electronics Engineering, Hacettepe University, Ankara, Turkiye {eozturk,uyanik,solen}@ee.hacettepe.edu.tr

and reliability of onboard sensing [25], [26]; this sensor-dependence makes them an effective and principled testbed for evaluating novel sensing modalities. We exploit this property by using Bug1, Bug2, and TangentBug as a structured evaluation framework to characterize the operational limits of the proposed soft antenna under realistic navigation conditions, demonstrating for the first time with a purely soft microfluidic antenna an autonomous robot executing multi-strategy reactive navigation using exclusively resistance-based soft antenna feedback, without rigid sensor elements or external sensor input.

The primary contributions of this paper are: (i) a systematic RLSE model selection procedure with explicit justification of model order and forgetting factor via leave-one-out cross-validation (LOOCV); (ii) first demonstration of autonomous soft-antenna-only navigation across three Bug algorithm variants; and (iii) a quantitative comparative analysis identifying conditions under which the soft antenna is demonstrably superior to ultrasonic sensing.

II. DESCRIPTION OF MATERIALS

A. Fabrication of the Soft Microfluidic Antennae

The proposed soft robotic antenna consists of two primary components: a flexible silicone rubber substrate and an electrically conductive carbon paste. The base structure is fabricated using addition-cured, room-temperature vulcanizing (RTV-2) silicone rubber. To achieve the necessary balance between structural integrity and sensitivity, two different hardness levels are used: Shore A 40 (medium) for structural support and Shore 00-30 (extremely soft) for enhanced flexibility. Electrical conductivity is achieved through the use of MG Chemicals carbon grease, which fills microchannels embedded within the silicone substrate. The fabrication process utilizes a two-step molding technique to create a sandwich structure. Initially, the harder silicone is poured into a 3D-printed mold and cured to form a stable base. Subsequently, the softer silicone is cast into a separate mold featuring a U-shaped microchannel pattern with dimensions of 1.5 mm in width, 195 mm in length, and 0.55 mm in height. After partial curing, these layers are aligned and bonded with additional silicone to ensure structural integrity. Conductive carbon grease is then injected into the channels, and electrical contact points are established by securing wires. The finished product, illustrated in Fig. 1, has a typical resistance range of 70–80$k\Omega$. The antenna's electrical behavior follows Pouillet's Law ($R = \rho \frac{l}{A}$). Resistance varies based on the bending direction: it decreases when flexed toward the microchannels and increases when bent outward. The manufacturing process requires 17 hours for curing and 30 minutes of preparation per sensor. While the sensor maintains operational functionality for approximately four months before the liquid conductive component is absorbed by the silicone matrix, its low material cost ($\sim$ \$1) makes it a highly scalable solution for mobile robotics. Mechanically, the high compliance of the antenna allows it to endure significant, reversible deformations without compromising sensing capability.

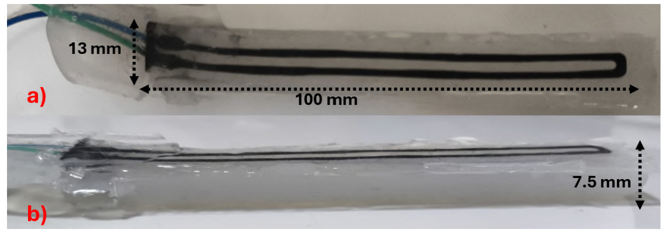

Fig. 1: Finalized soft robotic antenna: a) top view indicating width/height, b) side view indicating thickness.

B. Testing Apparatus for Sensor Characterization

To evaluate the performance of the soft microfluidic antenna, a specialized testing infrastructure and a mobile robotic platform were developed. A dedicated test platform was designed to validate the sensor's response under controlled conditions. As shown in Fig. 2, the setup consists of a linear guide that allows a test car to move in a single dimension against a 3D-printed wall surface. This wall features a predefined sinusoidal profile with a length of 70 cm and a peak-to-peak amplitude of 1.5 cm. The test car is equipped with a microcontroller and a voltage divider to regulate its motion and facilitate real-time data collection. To establish a ground truth for distance measurements, an ultrasonic sensor is mounted directly beneath the soft antenna's contact point, enabling a direct comparative analysis between the two sensing modalities at a sampling rate of 100 Hz.

The autonomous robot utilized for the evaluation of the soft microfluidic antenna features a 3D-printed PLA body equipped with a differential drive system, where two rear DC motors provide thrust and a front caster wheel ensures stability and turning (Fig. 3). Two dedicated sensor holders are mounted on the chassis: one at the front for obstacle detection and another on the front-right for wall-following tasks. The electronic system is centered around an Arduino MEGA 2560 microcontroller, which receives resistance-based analog signals from the soft antenna via its built-in ADC to determine bending-induced variations. Wireless communication for real-time positional data and localization is handled by an XBee module, while the entire system is powered by two independent pairs of Sony VTC6 18650 batteries to isolate motor noise from the control electronics.

Experiments were conducted within a controlled test environment, where an image-based localization system tracks the robot's position through color-coded markers. The control architecture, illustrated in the schematic in Fig. 4, is programmed in Simulink using MATLAB's Run on Target

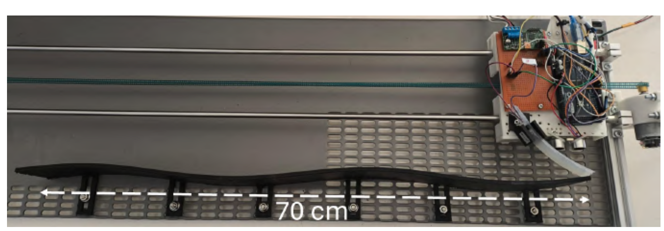

Fig. 2: Characterization apparatus: Test car and linear guide on a 3D-printed sinusoidal wall.

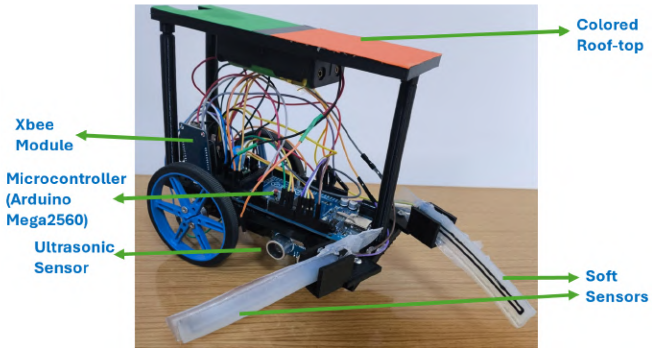

Fig. 3: Autonomous mobile robot: hardware configuration and sensor mount locations.

Hardware support to allow for real-time debugging and block-diagram-based logic. Within this framework, a PID controller adjusts motor thrust based on the error between the antenna's measured distance and a set reference, operating at a control frequency of 20 Hz to guide the robot during navigation.

III. SENSOR CHARACTERIZATION AND MODELLING

The frequency response and time-domain characteristics of the soft sensor were established by utilizing a known wall profile as ground truth. Building upon this foundation, the characterization process employed an ultrasonic sensor as a reference for the system identification of the soft sensor. Three distinct test runs were conducted using a single soft robotic antenna and an ultrasonic sensor against a sinusoidally varying wall surface consisting of three periodic cycles. To eliminate the influence of transient response effects, data from the initial cycle was discarded. The soft sensor measurements were processed by subtracting the mean value and normalizing the results to represent the percentage

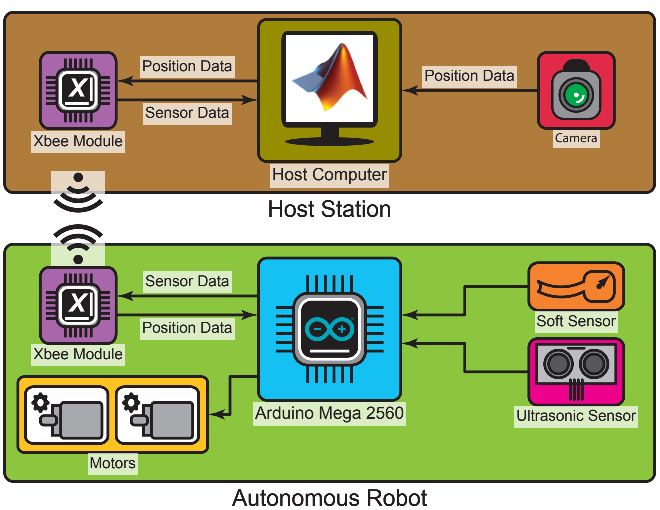

Fig. 4: Control system schematic: Communication and feedback loops between host station and robot. The Arduino and MATLAB logos are trademarks of their respective owners. Their use in this figure is for illustrative purposes only and does not imply endorsement by Arduino or MathWorks.

change in resistance. Each experimental trial served as an input-output dataset for a RLSE algorithm aimed at deriving a model for depth estimation [22]. In this configuration, the soft sensor data was treated as the system input, while the ultrasonic sensor data served as the target output for training. The training dataset used for this identification process is visualized in Fig. 5.

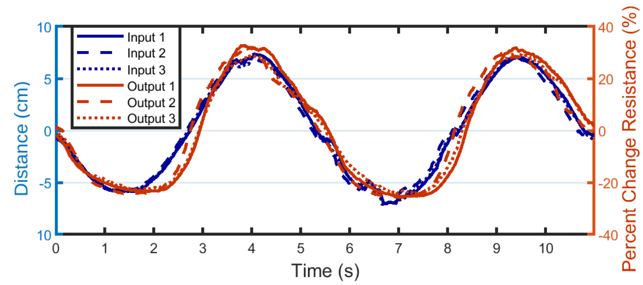

Fig. 5: Training dataset for RLSE: Normalized resistance input versus ultrasonic distance output.

To enhance the model's generalization capabilities, a LOOCV method was implemented. In each iteration of this process, one test run was designated for validation, while the mean of the remaining two runs served as the training set. A fifth-order RLSE model was ultimately selected after an evaluation of multiple system orders and forgetting factors. A final forgetting factor of 0.98 was chosen to achieve an acceptable performance. The results of this training, illustrated in Fig. 6, demonstrate the high degree of correlation between the estimated depth values derived from the soft sensor and the actual measurements from the ultrasonic sensor. The root mean square (RMS) error between the estimated and actual distances was found to be 1.28% in the first trial, 0.22% in the second, and 1.77% in the third. This calibrated model was then integrated into the autonomous robot's control framework for real-time navigation.

IV. CASE STUDY: IMPLEMENTING BUG ALGORITHMS WITH SOFT SENSORS

Bug algorithms are reactive path-planning strategies used in robotics for obstacle avoidance and goal-directed navigation in environments where prior obstacle mapping is unavailable. These algorithms guide a robot toward its target while dynamically adapting to obstacles through simple, sensor-based behaviors. To evaluate the efficacy of the proposed soft robotic antenna, experiments were conducted using Bug1, Bug2, and TangentBug algorithms within a

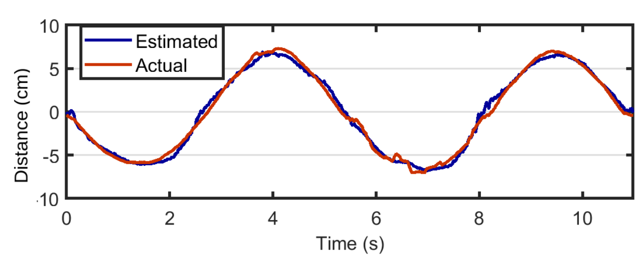

Fig. 6: RLSE validation results: Comparison of estimated depth and ground truth measurements.

controlled 2×2 meter test environment containing strategically placed obstacles. The experimental setup, including the varying navigation paths generated by each algorithm as the robot moves from its start position to the target, is illustrated in Fig. 7. Although positional data was available for localization, the robot relied exclusively on feedback from the soft antenna for distance measurement and obstacle avoidance.

A. Navigation Logic and Implementation

Obstacle detection was managed by a front-mounted soft antenna serving as a bumper sensor. Upon physical contact with an obstacle, the antenna's resistance drops, signaling the microcontroller to transition from goal-seeking to wall-following mode. During the wall-following phase, the robot maintains a consistent distance from the obstacle by monitoring resistance readings exclusively from the right-mounted soft antenna. A feedback-based PID control algorithm regulates this distance using the soft antenna's resistance as the sole feedback signal — the ultrasonic sensor, while physically present on the platform, is deliberately excluded from the control loop and used only for offline performance comparison against the soft antenna estimates. If resistance exceeds a predefined threshold (indicating the robot is moving away from the wall), the trajectory is adjusted to the right; if it falls below the threshold, the robot adjusts to the left. The three algorithms were implemented as follows: With **Bug1**, the robot moves toward the target until an obstacle is detected, then follows the entire perimeter of the obstacle

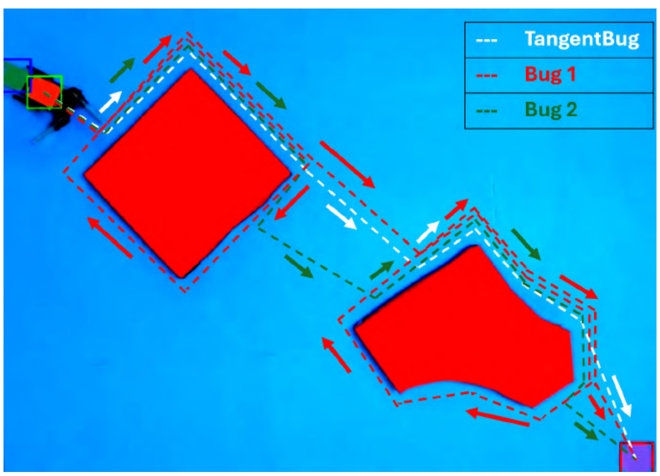

Fig. 7: Experimental navigation paths in the 2×2 m test arena containing two irregularly shaped obstacles. The robot starts from the upper-left and navigates toward the target (bottom-right, purple marker). White dashed lines and arrows indicate the TangentBug trajectory, which switches between boundary-following and direct navigation as soon as line-of-sight to the target is established. Red dashed lines and arrows indicate the Bug1 trajectory, which circumnavigates the full perimeter of each obstacle before resuming the direct path. Green dashed lines and arrows indicate the Bug2 trajectory, which leaves the obstacle boundary as soon as the robot re-aligns with the start-to-goal line.

before resuming its direct path toward the goal. The strategy of **Bug2** improves efficiency by allowing the robot to leave the obstacle's boundary as soon as it re-aligns with the direct trajectory from its starting position to the target [23]. **TangentBug** refines navigation by continuously evaluating line-of-sight availability to the target. It initially follows the boundary but switches back to direct navigation as soon as a clear path to the goal is established based on the robot's heading angle [24].

B. Comparative Analysis of Sensor Performance

The experimental results visualized in Fig. 8, Fig. 9, and Fig. 10 demonstrate the real-time efficacy of the soft antenna across the three navigation strategies. The performance is analyzed through the correlation of three data streams: the front-mounted bumper sensor, the right-mounted wall-following sensor, and the ultrasonic reference. In the Bug1 trial (Fig. 8), the recorded execution time is significantly longer as the robot must circumnavigate the entire obstacle perimeter. The Bumper Sensor Data clearly marks two distinct contact events where resistance drops sharply (below -50%), signaling the transition to wall-following mode. During the subsequent 10-second analysis window (50s to 60s), the Soft Sensor Distance Estimation aligns closely with the reference distance of 7.4 cm. However, the ultrasonic sensor consistently records distances 1–2 cm longer than the soft sensor. This is attributed to the soft sensor maintaining continuous physical contact with the wall, whereas the ultrasonic sensor may lose direct detection or suffer from angular misalignment, such as a slight downward tilt, leading to overestimated distances. The Bug2 trial (Fig. 9) exhibits a more efficient trajectory, reflected in the shorter time scale. The Soft Sensor Data in Fig. 9 shows a high-frequency ”wavy” pattern during the wall-following phase (between 10s and 25s). This phenomenon occurs when the robot maneuvers around corners; as the antenna momentarily loses contact, the resistance rises abruptly, creating a sharp spike in the estimated distance. Once contact is re-established, the resistance drops immediately, resulting in the characteristic fluctuations observed in the recorded signals. In the TangentBug implementation (Fig. 10), the robot frequently switches between boundary tracking and direct navigation. During these transitions, the soft antenna provides a more continuous proximity signal until the physical break of contact occurs. The reference distance during wall-following remains set to a resistance value corresponding to 7.4 cm, and the data illustrates the contact points of the bumper sensor with the obstacle, highlighting the effectiveness of the strategy in transitioning between modes. Furthermore, the ultrasonic sensor frequently registered void measurements (defaulting to 10 m) when maneuvering around corners or when not actively following a wall. In contrast, the soft antenna provided more stable proximity feedback, though it exhibited characteristic ”wavy” patterns caused by momentary losses of contact and subsequent abrupt resistance changes. Despite these transient fluctuations, the strong correlation between the two sensing modalities confirms that the soft antenna is an effective and

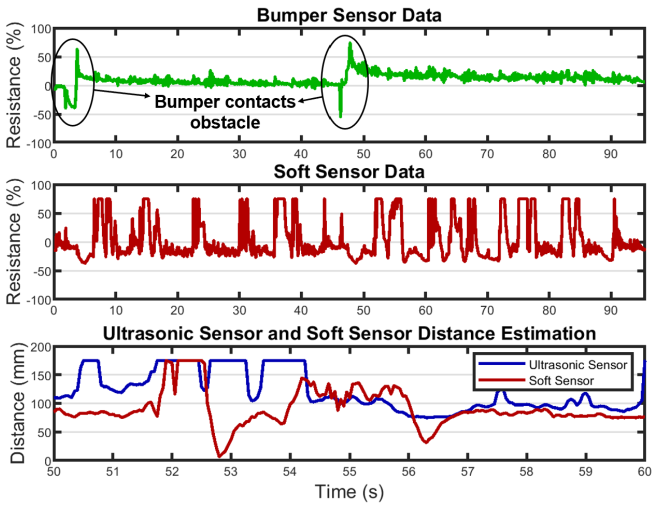

Fig. 8: Sensor performance during Bug1 navigation. Top: bumper antenna resistance, with two distinct contact events (circled) marking transitions to wall-following mode. Middle: right-mounted soft antenna resistance during full obstacle perimeter traversal ($\sim$ 90 s total). Bottom: filtered distance estimates over a representative 10-second wall-following window (50–60 s), showing close agreement between the soft sensor (red) and ultrasonic reference (blue), with the ultrasonic sensor consistently reading 1–2 cm longer due to angular misalignment and loss of direct wall detection.

resilient alternative for real-time depth perception.

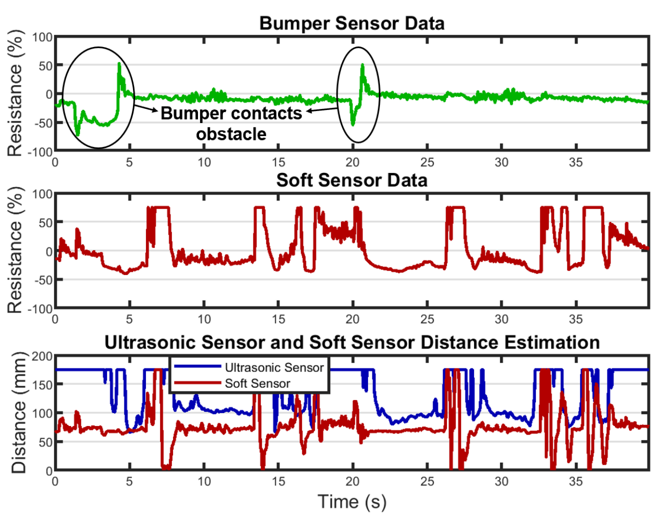

Fig. 9: Sensor performance during Bug2 navigation. Top: bumper antenna resistance, with two obstacle contact events (circled) triggering boundary-following. Middle: right-mounted soft antenna resistance showing characteristic high-frequency fluctuations as the antenna repeatedly loses and re-establishes contact at corners. Bottom: filtered distance estimates over the full trial ($\sim$ 38 s), where the soft sensor tracks wall proximity continuously while the ultrasonic sensor frequently saturates to its maximum range during corner maneuvers.

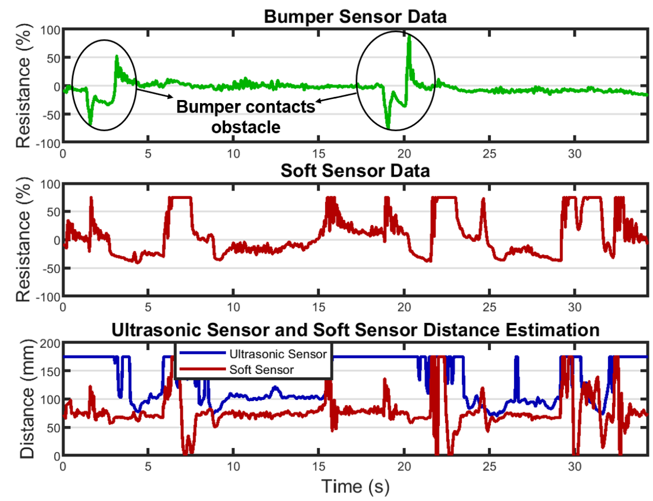

Fig. 10: Sensor performance during TangentBug navigation. Top: bumper antenna resistance, with two contact events (circled) initiating boundary-following phases. Middle: right-mounted soft antenna resistance reflecting frequent transitions between wall-following and direct line-of-sight navigation. Bottom: filtered distance estimates over the full trial ($\sim$ 33 s), demonstrating that the soft sensor maintains continuous proximity feedback across mode switches, while the ultrasonic sensor registers repeated void measurements when not actively facing a wall.

V. CONCLUSIONS

This paper presents a low-cost, bio-inspired soft robotic antenna for close-proximity distance perception and demonstrated its integration into an autonomous navigation system executing Bug1, Bug2, and TangentBug algorithms. Fabricated from a stretchable silicone elastomer with embedded conductive carbon paste microchannels, the sensor provides reliable resistance-based distance feedback at a material cost of approximately \$1 per unit. A fifth-order recursive least squares estimation (RLSE) model — with model order and forgetting factor selected through systematic leave-one-out cross-validation (LOOCV) — was shown to accurately estimate wall distance with RMS errors below 1.77% relative to ultrasonic ground truth. Across all three navigation algorithms and all trials, the robot successfully reached the goal using exclusively soft antenna feedback, without any external sensor input. A key finding that distinguishes this work from prior art is the identification of operating conditions in which the soft antenna is not merely a cost-effective substitute for rigid sensing, but a genuinely superior modality. During corner maneuvers, ultrasonic sensors frequently registered void measurements due to angular beam misalignment, while the soft antenna maintained continuous and stable proximity feedback. This contact-based immunity to acoustic reflection artifacts establishes soft antennas as a primary sensing candidate — not a fallback — for close-proximity navigation in geometrically complex environments such as narrow corridors and sharp-cornered passages.

The results presented in this work establish the soft microfluidic antenna as a reliable and cost-effective sensing modality for close-proximity navigation, with performance that compares favorably to — and in corner-following scenarios surpasses — conventional ultrasonic sensing. As with any first-generation soft sensing platform, several avenues remain open for further development: the operational lifespan of several months, while sufficient for laboratory and short-term field deployment, is governed by the gradual absorption of carbon grease into the silicone matrix and can be extended through material substitution. The fifth-order RLSE model captures the sensor's dominant linear dynamics with high accuracy, and its residual approximation error at large deflection angles (beyond ±30°) motivates the development of nonlinear model extensions. Finally, bench-based characterization, while controlled and reproducible, does not expose the sensor to the full range of contact conditions encountered during live navigation — a gap that provides a clear and tractable direction for future work.

Building on these strengths, future work will address three open directions. First, the characterization paradigm will shift from bench testing to in-situ system identification: antenna resistance data collected during live robot navigation will serve as training input, with camera-based localization providing ground-truth distance measurements as the target output. This will expose the sensor to the actual friction, vibration, and variable contact angles present during deployment — conditions that bench-based characterization does not capture — and will enable a rigorous three-way accuracy assessment comparing soft antenna, ultrasonic, and camera ground truth. Second, that in-situ dataset will be used to train and compare the current linear RLSE model against a Long Short-Term Memory (LSTM) network, which is expected to better capture temporal dependencies and hysteresis effects at large deflection angles; a sensitivity analysis of the forgetting factor will also be conducted to characterize model robustness. Third, the evaluation will be extended to more geometrically demanding environments — including narrow corridors and sharp-cornered passages — using multiple independently fabricated antenna specimens to assess manufacturing variability and trial-to-trial repeatability, and the best-performing sensor model will be integrated into more sophisticated navigation algorithms such as Vector Field Histogram (VFH) or Artificial Potential Field (APF).

References

[1] T. J. Prescott, M. E. Diamond, and A. M. Wing, Active touch sensing, Phil. Trans. R. Soc., vol. 366, pp. 2989-2995, 2011.

[2] E. M. Staudacher, M. Gebhardt, and V. Dürr, Adv In Insect Phys, vol. 32, pp. 49-205, 2005.

[3] J. M. Camhi, E. N. Johnson, High-frequency steering maneuvers mediated by tactile cues: Antennal wall-following in the cockroach, J. Exp. Biol., vol. 202(5), pp. 631-643, 1999.

[4] C. Schutz, and V. Durr, Active tactile exploration for adaptive locomotion in the stick insect, Phil. Trans. R. Soc., pp. 2995-3005, 2011.

[5] S. Massashi, Serpentine locomotion with robot snakes, IEEE Journal of Control System, vol. 22, pp. 344-356, 2002.

[6] S. Soyguder, and H. Alli, Design and prototype of a six-legged walking insect robot, Ind Rob, vol. 34(5), pp. 412-422, 2007.

[7] A. Alessi, A. Sudano, D. Accoto, and E. Guglielmelli, Development of an autonomous robotic fish, .4th IEEE RAS and EMBS International Conference on Biomedical Robotics and Biomechatronics (BioRob), pp. 1032-1037, June, 2012.

[8] I. Uyanik et al., Experimental validation of a feed-forward predictor for the spring-loaded inverted pendulum template, IEEE Transactions on Robotics, vol. 31(1), pp. 208-216, 2015.

[9] C. Fiazza et al., Biomimetic mechanical design for soft-bodied underwater vehicles, Proc. of IEEE Oceans, pp. 1–7, 2010.

[10] C. Laschi, B. Mazzolai, M. Cianchetti, L. Margheri, M. Follador, and P. Dario, A soft robot arm inspired by the octopus, Adv Robot, vol. 26(7), pp. 709–727, 2012.

[11] D. S. Shah, J. P. Powers, L. G. Tilton, et al., A soft robot that adapts to environments through shape change, Nat Mach Intell vol. 3, pp. 51–59, 2021.

[12] N. Cowan, E. Ma, M. Cutkosky, and R. Full, A biologically inspired passive antenna for steering control of a running robot, Robotics Research, The Eleventh International Symposium, vol. 15, pp. 541-550, 2003.

[13] A. G. Lamperski, O. Y. Loh, B. L. Kutscher, and N. J. Cowan, Dynamical wall following for a wheeled robot using a passive tactile sensor, Proceedings of the 2005 IEEE International Conference on Robotics and Automation, pp. 3838-3843, 2005.

[14] J. Lee, S. N. Sponberg, O. Y. Loh, A. G. Lamperski, R. J. Full, and N. J. Cowan, Templates and anchors for antenna-based wall following in cockroaches and robots, IEEE Transactions on Robotics, vol. 24(1), pp. 130-143, 2008.

[15] S. K. Yildiz, R. Mutlu, G. Alici, Position control of a soft prosthetic finger with limited feedback information, 2018 IEEE/ASME International Conference on Advanced Intelligent Mechatronics (AIM), pp. 700-705, 2018.

[16] H. Ren, L. Yang, H. Y. Chang et al., A robust and omnidirectional-sensitive electronic antenna for tactile-induced perception. Nat Commun 16, 3135, 2025.

[17] D. Zhu et al., Self-powered bionic antenna based on triboelectric nanogenerator for micro-robotic tactile sensing, Nano Energy, Volume 114, 2023.

[18] Y. Zhou, M. Ju, and G. Zheng, Closed-loop control of soft robot based on machine learning, 2019 Chinese Control Conference (CCC), pp. 4543-4547, 2019.

[19] R. K. Katzschmann et al., Dynamically closed-loop controlled soft robotic arm using a reduced order finite element model with state observer, 2019 2nd IEEE International Conference on Soft Robotics (RoboSoft), pp. 717-724, 2019.

[20] Z. J. Xu, J. He, D. Aydan et al., A robust antenna provides tactile feedback in a multi-legged robot, arXiv:2603.07795, 2026.

[21] O. Demir, E. Ozturk, E. Sayar, I. Uyanik and S. K. Yildiz, "Characterization of Soft Robotic Antenna for Close-Proximity Distance Perception," 2023 31st Signal Processing and Communications Applications Conference (SIU), Istanbul, Turkiye, 2023, pp. 1-4.

[22] Ljung L., System identification: theory for the user. Prentice Hall PTR, New Jersey, A.B.D., 2012.

[23] Lumelsky, V.J., Stepanov, A.A., Path-planning strategies for a point mobile automaton moving amidst unknown obstacles of arbitrary shape, Algorithmica, vol. 2, pp. 403–430, 1987.

[24] Kamon I, Rimon E, Rivlin E.,Tangentbug: A range-sensor based navigation algorithm, The International Journal of Robotics Research, 17(9), 934–953, 1998.

[25] K. N. McGuire, G. C. H. E. de Croon, and K. Tuyls, A comparative study of bug algorithms for robot navigation, Robotics and Autonomous Systems, vol. 121, p. 103261, 2019.

[26] J. Ng and T. Bräunl, Performance comparison of bug navigation algorithms, Journal of Intelligent and Robotic Systems, vol. 50, pp. 73–84, 2007.